Tracking and monitoring fin whales offshore northwest Spain using passive acoustic methods

J. Fisher[1], T. A. Minshull[1*], P. R. White[2], B. Tian[2] and G. Bayrakci[3]

1. School of Ocean and Earth Science, University of Southampton, National Oceanography Centre Southampton, European Way, Southampton SO14 3ZH.
2. Institute of Sound and Vibration Research, University of Southampton, Highfield, Southampton SO17 1BJ, UK
3. National Oceanography Centre, European Way, Southampton SO14 3ZH.

*Correspondence to: tmin@noc.soton.ac.uk

Abstract:

Fin whales produce regular vocalizations with a dominant frequency of c. 20 Hz, similar to that of large airgun sources used in marine seismic surveys. Thus these vocalizations may be recorded on ocean bottom seismometers (OBS) or hydrophones (OBH) deployed during such surveys. We used data recorded by an array of 72 OBS/H with 4-6.5 km spacing, deployed offshore northwest Spain during June-August 2013, to study fin whale movements in this area. Whale vocalizations were identified automatically using signal processing techniques and localized using time delay estimates between several instruments. Airgun shooting took place during the deployment period, but we found no evidence for a correlation between vocalization detection rate and the presence or absence of shooting. Our analysis focused on six fin whale tracks identified during this period. Uncertainties in depth lead to poor confidence intervals, preventing effective analysis of diving behavior for the identified tracks. In the horizontal plane, the localizations had a higher degree of confidence. Use of a Kalman filter resulted in smoother tracks. Mean swim velocities range from 2 to 15 km/hr, and the animals traveled distances of 1.5-15 km in the periods analyzed.

Keywords: ocean acoustics, marine mammals, acoustic tracking

1. Introduction

Passive acoustic monitoring

Passive acoustic monitoring (PAM) has been used increasingly to study cetaceans because studying marine life from visual observations can be challenging [*Moore et al.*, 2006]. Visual monitoring is limited to daylight hours and periods of good weather, and it is difficult to infer animal behavior from brief and rare sightings. Cetaceans use sound for communication, navigation and locating prey [*Nowacek et al.*, 2016], and it has become clear that detecting their vocalizations is an effective monitoring method that can complement visual observations [*Mellinger et al.*, 2007]. PAM can be conducted without interfering with the cetaceans in their natural environment over extended periods of time [*Zimmer*, 2011]. Recent technological advances mean that acoustic surveys can be conducted at lower expense and over greater periods of time than ever before. Here we use fixed hydrophone PAM to study fin whales (*Balaenoptera physalus*) from their vocalizations (calls). This is a highly efficient technique because at certain times of the year fin whales vocalize frequently and the sound can be detected and recorded at distances of tens of kilometers [*McDonald et al.*, 1995; *Stafforda et al.*, 2007].

Typically hydrophones are used for passive acoustic surveys and are either towed behind a vessel or fixed in place on the sea floor [*Mellinger et al.*, 2007]. The use of fixed hydrophones can be subdivided into cabled long-term deployments [*Au and Lammers*, 2016; *Clark et al.*, 2019; *McCarthy et al.*, 2011], where data is returned to shore in real-time (or near real-time) and shorter term deployments of autonomous recorders, that need to be retrieved for data collection [*Nguyen Hong Duc et al.*, 2021; *Wiggins and Hildebrand*, 2007]. In some instances, as is the case in the work detailed here, the instruments are deployed for an objective unrelated to PAM and the analysis to obtain information regarding marine mammals is secondary [*Clark*, 1995]. The use of multiple instruments with close spacing allows vocalizations to be detected on several hydrophones and thus to be used to track the source of the sound [*Zimmer*, 2011]. Ocean bottom seismometers/hydrophones (OBS/H) provide one type of instrument from which make these opportunistic observations of marine mammals [*Harris et al.*, 2013; *Harris et al.*, 2018; *Iwase*, 2015; *Matias and Harris*, 2015; *Rebull et al.*, 2006]. Such instruments provide a well-suited platform to observe deep-water marine mammals that produce low-frequency sounds. In particular, the distinctive, high intensity calls of fin whales provide an obvious candidate for study.

By using techniques developed for earthquake seismology, even a single OBS can be used to estimate range to a vocalizing animal [*Harris et al.*, 2013]. A network of devices can be used to improve the localization accuracy, for example, using the time difference of arrivals [*Dunn and Hernandez*, 2009]. In addition, it has been demonstrated that surface reflections can be used to estimate the depth of a calling whale [*Pereira et al.*, 2020b]. These data can be used for marine management planning and to obtain ecologically significant parameters, such as animal density [*Harris et al.*, 2018].

Fin whale vocalizations

Fin whales vocalize within the frequency range 15-142 Hz [*Edds*, 1988; *Širović et al.*, 2007; *Thompson et al.*, 1992; *Watkins et al.*, 1987]. The low frequency means that their calls can propagate large distances and are likely to be used for communication or navigation [*Croll et al.*, 2002; *Edds-Walton*, 1997; *Sirovic et al.*, 2013]. The most commonly studied fin whale call is the "20 Hz call" [*Hatch and Clark*, 2004] that here will be considered as the "classic" call and has maximum energy at 21 Hz [*Clark et al.*, 2002]. These calls have a distinctive down sweep in frequency [*Locke and White*, 2011] which can be obscured at longer ranges where reverberation and attenuation can make this structure difficult to observe. This classic call typically has a signal energy of 40 J, a signal length of approximately 1 s, and a source level measured using OBSs of c. 189 dB re 1 μPa m [*Weirathmueller et al.*, 2013; *Zimmer*, 2011].

The calls are typically emitted in trains within which there are interspersed "backbeat" calls which are upweeps that are shorter in duration than the classic calls, have a narrower bandwidth and are approximately 1 Hz lower in frequency (Fig. 1). These sequences of calls may vary in duration and call combinations depending on the activity or social behavior of the fin whale [*Edds-Walton*, 1997; *McDonald et al.*, 1995]. Variations in call trains also have been observed between different fin whale populations and may develop over time. Intervals between consecutive classic calls, the so-called inter-note interval (INI), typically range between 7 and 26 seconds [*Watkins et al.*, 1987]. For example, mean intervals are c. 13 s in the eastern North Atlantic but c. 15 s in the western Mediterranean, indicating the presence of two distinct populations [*Castellote et al.*, 2012]. Intervals longer than the normal INIs are referred to as rests, and typically last for several minutes

[*Watkins et al.*, 1987]. These rests correspond to periods when the whale surfaces to breathe, or dives deep, and the typical rest periods for these activities are 150 s and 600 s, respectively [*McDonald et al.*, 1995]. In cases where calling ceases for over 20 minutes, the silent period is referred to as a “gap” [*Watkins et al.*, 1987].

Baleen whales commonly migrate between summer feeding grounds at high latitudes and winter breeding and calving grounds at lower latitudes [*Kellogg*, 1929], but a wide range of migratory behaviors has been observed [*Geijer et al.*, 2016]. Detection of vocalizations in temperate latitudes is strongly seasonal, with peak activity in the winter months and limited activity in the summer [*Pereira et al.*, 2020a; *Watkins et al.*, 1987]. This variation may be linked both to migration patterns and to seasonal variations in behavior associated with the mating season [*Oleson et al.*, 2014]. However, a tagging study near the Azores that focused on the months of March to May in 2010-2012 suggested that tagged animals were foraging whilst on a northward migration towards Greenland [*Silva et al.*, 2013].

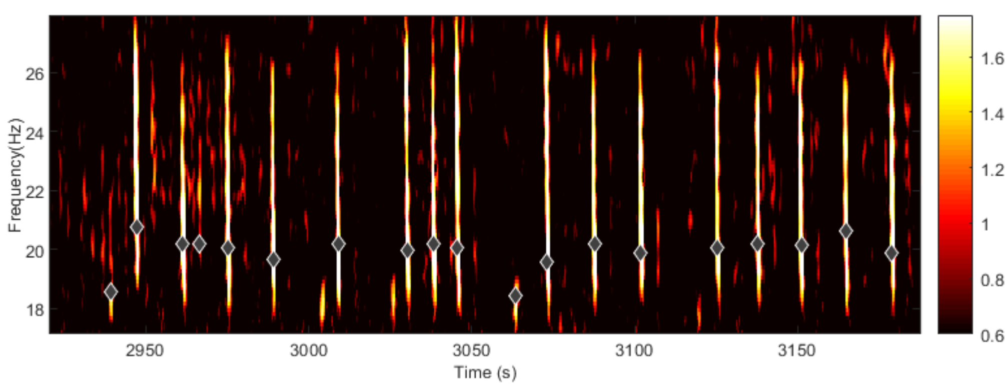

Figure 1: Normalized spectrogram illustrating a typical fin whale call pattern observed in our dataset. The normalization is described in the text. Broader-band signals are classic calls and narrower-band signals are backbeats. Grey diamond markers indicate call detections by our automated algorithm.

Data available for this study

Our dataset comes from 50 four-component ocean bottom seismometers (OBSs) [*Minshull et al.*, 2005] and 28 ocean bottom hydrophones (OBHs) deployed on the seabed in c. 5 km water depth during May-August 2013 as part of the Galicia3D study (Fig. 2), which was focused on the structure of the crust and uppermost mantle in a region where the crust is highly stretched [*Bayrakci et al.*, 2016; *Schuba et al.*, 2018]. The deployment covered the summer period when fewer fin whale vocalizations are expected, and indeed fewer were observed during an OBS deployment offshore Iberia to the south of our study area [*Pereira et al.*, 2020a]. However, the deployment was within an area where fin whales have been previously detected acoustically in the summer months [*Rebull et al.*, 2006]. The instruments were distributed in a 18 x 4 grid with an east-west spacing of c. 6.5 km and a north-south spacing of c. 4 km, to cover an area of 80 km x 25 km, with an additional six instruments on a line extending further west that provided limited useful data for our study. Several OBS/H were not retrieved or returned with no usable data, leaving 44 OBSs and 26 OBHs that could be used for our study. OBSs recorded at a sample rate of 250 Hz and OBHs at 200 Hz, with the OBS data being down-sampled to 200 Hz, so that a consistent sample rate was used for all data. Differences in hardware meant that the OBHs and some OBSs recorded for the entire period of their deployment, while other OBSs lost battery power before recovery. The survey involved active airgun shooting during the periods 5^{th}-23^{rd} June (Julian days 156-174) and 16^{th}-31^{st} July (Julian days 197-212), with the survey vessel returning to port in between these periods because of an engine failure. For this study, we used hydrophone data recorded from 5^{th} June to 12^{th} August (Julian days 156-224). Instrument clocks were synchronized with Universal Time on deployment and recovery, and a linear clock drift assumed between these times. Instruments used for detection and location had a mean drift rate of 4 ms/day and the maximum rate was 25 ms/day. If such synchronization was not possible or the clock drift rate was larger, the data were not used. Instrument locations on the seabed were determined using the travel-times of airgun shots [*Bayrakci et al.*, 2016].

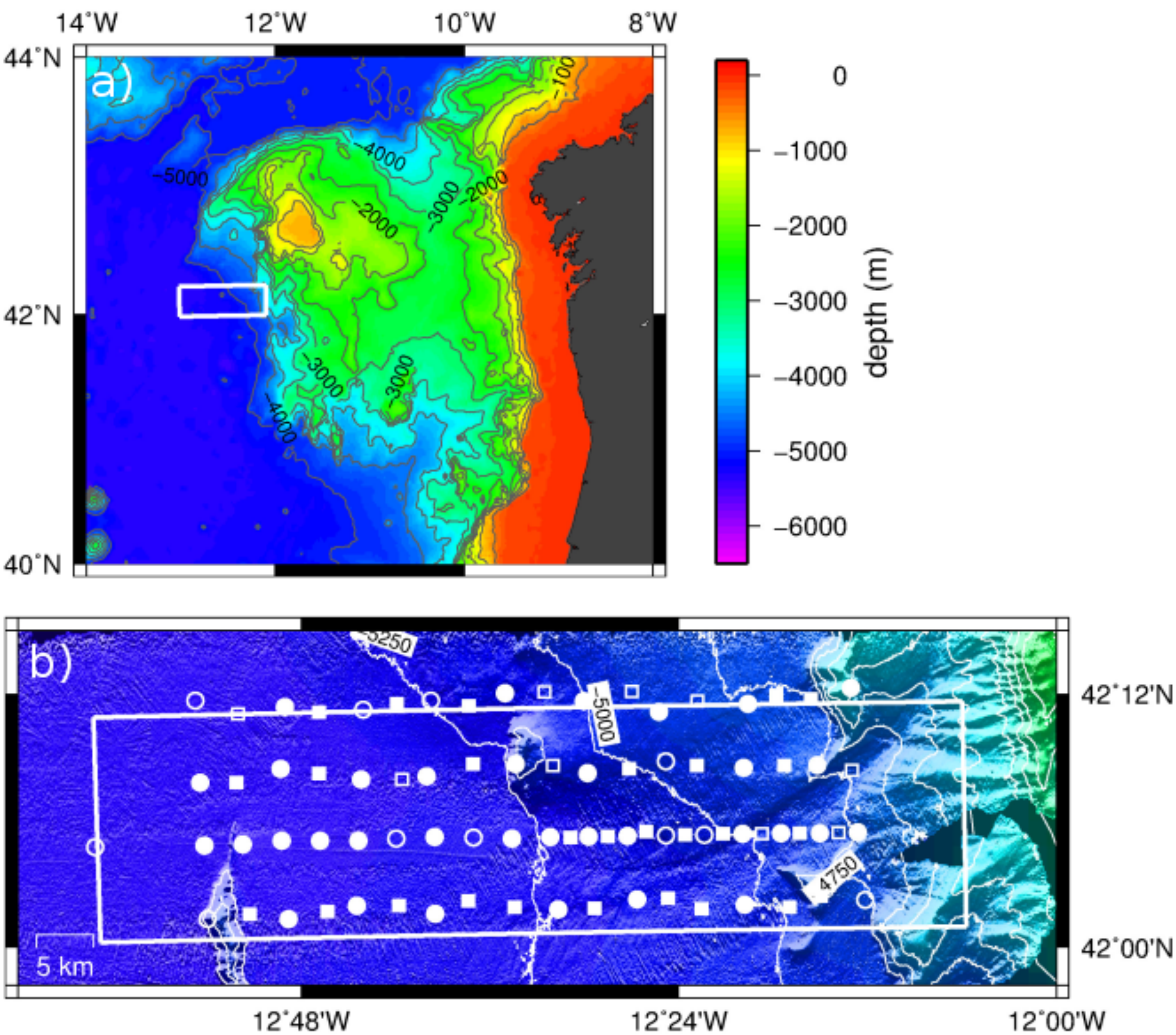

Figure 2: (a) White box marks survey area on the Deep Galicia Margin. Bathymetry is from Smith and Sandwell (1997). (b) Swath bathymetric grid of survey area. Circles mark OBS locations and squares mark OBH locations, with filled symbols marking instruments that provided usable data for this study. White box marks area of airgun shooting.

2. Methods

Call detection

The recorded data were first converted to day-long WAV files, to allow for audio playback at an increased speed that renders the vocalizations audible to the human ear. Our analysis is based on the spectrogram, which is computed using a Hanning window of 512 samples, with an overlap of 87.5% (yielding frequency and time resolutions of 0.4 Hz and 0.32 s, respectively). The spectrogram is normalized based on a robust estimate of the power spectrum, which is computed using the median of the spectrogram values in each frequency bin [*Leung and White*, 1998]. The normalized spectrogram is obtained by dividing each value in the original spectrogram by the power spectrum at the corresponding frequency.

In addition to fin whale calls, the instruments recorded the shots of the seismic survey, some earthquakes, and noise from passing vessels, as well as ambient noise due to ocean waves. To reduce errors in the detection of the fin whale vocalizations, filtering can be used to isolate the specific frequency band to promote successful detections. In band and outer band frequency ranges were determined to optimize the filtering of the data. To detect the whale vocalizations the mean energies in three bands are computed based on the normalized spectrogram. The three bands are the *in-band* which are the range of frequencies where a fin whale 20 Hz call is expected to appear, in this case 15-30 Hz is used, and two *out-bands* one covering the frequency range below the in-band, i.e. <15 Hz, and one above the in-band, i.e. >30 Hz. For each one-hour block, the energies in each band are calculated as the mean of the normalized spectrogram in the two bands. A detection is only made if the energy is above the threshold of 5 in the in-band but below the threshold of 5 for both of the out-bands. This threshold value of 5 was determined by testing various values on a small subset of data which had been manually annotated. This dual criterion is used to eliminate false alarms from sounds that occur across a range of frequencies and are not restricted to the 15-30 Hz range.

Delay estimation

The localization process for a source is based on estimation of the time differences of arrivals (TDoAs) measured between different instruments. The TDoAs represent the delays of the signals observed on the different sensors. For an array of N sensors, there are two broad strategies that can be adopted regarding which TDoAs to compute. The first is to compute the TDoAs between all possible pairs of sensors [*White et al.*, 2006], which results in $N(N\text{-}1)/2$ TDoAs. The second is to select a reference sensor and compute the TDoAs only between the reference sensor and each of the other sensors, which requires only N-1 values to be computed. The second approach has the advantage of reducing the computational load because of the smaller number of TDoAs that are computed. Further, in principle, one can compute all the possible TDoAs from the subset computed relative to a reference sensor. However, the first approach is more robust to estimation errors because there is some redundancy in the approach.

The calculation of the TDoAs is most commonly based on a cross-correlation [*Knapp and Carter*, 1976]:

$$\hat{R}_{f_1 f_2}(\tau) = \frac{1}{T - |\tau|} \int_0^T f_1(t - \tau) f_2(t) dt \tag{1}$$

where f_1 and f_2 are the time series and T is their duration, and the value of the lag, τ, at which the cross-correlation is maximum was determined and used as the estimate of the TDoA. The correlation can be computed based on the raw acoustic data or using the time series of a metric derived from the acoustic data. If the acoustic data is to be used in the correlation function then the underlying assumption is that the difference between the acoustic signals on two instruments is a simple delay and an amplitude scaling. This may not be true for a variety of reasons, including: complexities in the propagation conditions (e.g. reflections), source directivity and noise. These approximations are more justifiable for sensors that are close to each other.

For pulsed signals, such as fin whale calls, we can regard the signal as consisting of two components. Borrowing terminology from the fields of communications, radar and sonar, we can refer to the carrier signal as being the frequency of each pulse (c. 20 Hz) and the modulation signal defining the shape of the pulses at frequencies of the order of 0.1 Hz. This decomposition provides two routes for computing the delays. The first is based on correlating the carrier waveforms, which potentially provides greater levels of precision, with the second being based on correlating the modulation waveform, which results in lower precision but greater robustness.

Here we describe methods based on the modulation function, which use the envelope of the waveform as an estimate of this modulation signal. To reduce the effect of noise, prior to computing the modulation function, two processes are adopted. First, out-of-band noise is removed by bandpass filtering the signals between 15 and 30 Hz. Then noise within the band of fin whale calls is reduced using a technique pioneered for speech enhancement, specifically power subtraction [*McAulay and Malpass*, 1980]. Following filtering and enhancement, the cross-correlation is calculated using the envelope of the signals. The envelope is computed using the analytic signal based on a Hilbert transform. The analytic signal, $f_a(t)$, is a complex representation of a signal $f(t)$ and is given by:

$$f_{\mathrm{a}}(t) = f(t) + i\tilde{f}(t) \quad (2)$$

where $\tilde{f}(t)$ is the Hilbert transform of $f(t)$ [*Marple*, 1999]. The envelope is then the magnitude of the analytic signal.

A potential problem with the cross-correlation approach is that the call trains have an INI that is nearly constant, so the computed cross-correlation functions have multiple peaks, separated by the INI. Thus the wrong peak may be selected to compute the TDoAs. This possibility is mitigated in two ways. Firstly, the natural variation in the INIs means that averaging across longer time intervals reduces the height of the secondary (false) peaks in the cross-correlation function, favoring the use longer time windows, which capture more of this natural variation. Secondly, the ambiguities generally correspond to unphysical time delays because the interval between calls is around 14 s, which corresponds to path length differences of roughly 20 km. This observation also provides a second motivation for choosing to correlate the modulation function rather than the carrier signal, since the ambiguous peaks observed for the carrier signals occur at much shorter path length distances (~0.05 s or 75 m) and are typically physically realistic, so much harder to eliminate.

The window length selected to compute the cross-correlation functions is a compromise. A long window reduces the potential problems of secondary peaks in the cross-correlation function and also increases the signal-to-noise ratio (SNR) of the peaks. A short window allows a greater number of independent localizations to be computed, but the reduced information produces low correlation peaks which are more readily masked by noise. A short window also decreases the influence of motion of the animal during the cross-correlation window, that will blur the main peak, introducing greater uncertainty in the TDoA estimates. This effect suggests a criterion for the maximum window length: that the animal's motion within a window should not result in a TDoA change that is greater than the width of the main correlation peak. The greatest possible change in the TDoA is twice the distance travelled by the whale divided by speed of sound: this would correspond to the whale swimming along the line connecting the two hydrophones, i.e., swimming and vocalizing at the bottom of the ocean (something that fin whales do not do). For that case, assuming a whale swimming at 10 km/hr and a width of the correlation peak of 1 s (the typical duration of the call), the corresponding window duration is 280 s. We used a value of 300 s, which based on the extremely conservative nature of the preceding calculation, is a realistic choice. These windows were overlapped by 50%. The TDoA estimate was assumed to correspond to a position in the middle of the time window. The effects of absolute propagation time were neglected, leading to a systematic position error of up to a few 10s of metres (depending on swim speed) that does not affect swim speed estimates.

The TDoA estimates were post-processed to remove outliers by examining the errors relative to a linear trend. Time delays were also displayed graphically and only used to determine tracks if they showed a smooth progression in time. We used the closest instrument to the whale as a reference and only computed the TDoAs between this instrument and all of the other instruments. An alternative approach woud be to compute TDoAs across all pairs of instruments which detect the whale.

Localization and tracking

Various methods have been used to localize the source of whale vocalizations from time delay estimates [*Baggenstoss*, 2011; *Rebull et al.*, 2006; *Wilcock*, 2012]. We used the method of *White et al.* [2006] to localize and track the whales. An inversion model from the time delays needs to be applied, and this is achieved with a maximum likelihood estimator by minimizing the weighted least squares cost function:

$$\Psi\big(\boldsymbol{s}(n)\big) = \sum_{k=2}^{N} \frac{\Big(\Delta_{1k}(n) - \mathrm{M}_{1k}\big(\boldsymbol{s}(n)\big)\Big)^2}{\sigma^2} \tag{3}$$

where $\boldsymbol{s}$ is the estimated source location of a discrete time *n*, Δ_{1k} is the estimated time delay between sensor 1 and sensor *k*, M_{1k} is the modelled delay between sensor 1 and sensor *k* and σ^2 the weighted variance of the time delays [*White et al.*, 2006]. For efficiency a linear sound speed model was adopted, where the speed of sound at the ocean surface is 1505 m/s and the vertical gradient is 0.017 /s. The gradient represents the change in hydrostatic pressure with increased depth for a constant temperature and salinity in the water column, corresponding to the deep isothermal layer [*Etter*, 1995]. This simplification allows rapid localization and reproduces correctly the flattening of propagation paths in the deep ocean, but overestimates the mean sound speed of c. 1520 m/s [e.g., *Davy et al.*, 2018] by c. 2%. When attempting the localization it is assumed that there is only one whale present, that the delay times are valid with no false detections and that there are no surface reflections or echoes present in the data. If for a given OBS and detection a direct path could not be computed, the delay time for that OBS and detection was not used. Manual checks were made on the INI to check that tracks used involved only one animal. The extension of this method to tracking multiple animals is a significant step, leading to the field of multi-target tracking [*Mahler*, 2004].

A minimum of four instruments are needed to successfully locate the source. For computational convenience the hydrophone locations were projected into Cartesian coordinates; the areas of interest were small enough to neglect the curvature of the Earth. The localization was achieved by minimizing the cost function (3) using a Nelder-Meade simplex method, implemented with random multiple initializations. A Monte Carlo method was employed to quantify the errors associated with noise processes. The depth at which fin whales vocalize is poorly characterized, with acoustic tag data suggesting that depths of up to 30 m [*Stimpert et al.*, 2015], so the algorithm was run both constrained such that the whale was assumed to be at the sea surface, and unconstrained such that its depth could correspond to anywhere in the water column. Prior knowledge of the depth distribution of vocalizing animals could usefully be incorporated into the method via a Bayesian framework.

Kalman filter

By constructing a sequence of localizations from a whale, one can form tracks of the whale motion during the time it is calling. Once localizations had been conducted for each sequential vocalization, the next procedure was to apply a Kalman filter to create a final animal track. The use of a Kalman filter estimates the movement parameter of the whales and presents the "most probable" whale track from the data. If the stochastic processes are Gaussian and the system is linear, then the Kalman filter represents an optimal estimator, both in the minimum mean squared sense and more generally as the Bayesian maximum *a posteriori* estimate of the state vector [*Bibby and Toutenburg*, 1977]. The Kalman filter predicts the motion of the fin whale whilst reducing noise with the associated measured points and relies upon a state-space model of the whale motion and measurement processes. A state-space model builds a representation of a system through defining a state vector; in this case the state vector is taken as containing the whale's position and velocity. The model here describes the whale's motion in either two or three dimensions. In the case of two dimensions the model is simplified by assuming that the animal only moves in a horizontal plane, i.e. the vertical motions can be neglected, which is valid if the diving depth of the whale is small compared to the water depth. In the following, we provide details of the two-dimensional model; the extension to three dimensions follows straightforwardly. The state vector, $\mathbf{x}_s(n)$, describing the whale's motion in two dimensions is given by:

$$\boldsymbol{x}_s(\boldsymbol{n}) = [\boldsymbol{x}(\boldsymbol{n}), \dot{\boldsymbol{x}}(\boldsymbol{n}), \boldsymbol{y}(\boldsymbol{n}), \dot{\boldsymbol{y}}(\boldsymbol{n})]^{\boldsymbol{t}} \tag{4}$$

where $(x(n),y(n))$ is the whale's position in the plane at time n and the dot notation is used to denote differentiation with respect to time.

This state-space model has two update equations, one describing the motion of the animal, i.e. how $\mathbf{x}_s(n)$ evolves with time, and the second the measurement process. The motion model is:

$$\mathbf{x}_s(n+1) = \mathbf{A}\mathbf{x}_s(n) + \mathbf{w}(n+1) \tag{5}$$

Here the linear transition matrix **A** describes the movement from time t_n to t_{n+1}, and $\mathbf{w}(n)$ represents stochastic processes driving the animal's motion. We used a "near constant velocity" model [*Li and Jilkov*, 2003] to define **A,** which is widely used in tracking problems, for example to track aircraft in radar applications, and a Gaussian white noise process for the vector $\mathbf{w}(n)$. According to this model the matrix **A** has the form:

$$\boldsymbol{A} = \begin{bmatrix} 1 & \Delta & 0 & 0 \\ 0 & 1 & 0 & 0 \\ 0 & 0 & 1 & \Delta \\ 0 & 0 & 0 & 1 \end{bmatrix} \tag{6}$$

where Δ is the interval between two samples. The model for measurements in this application is straightforward: specifically, the measurements are assumed to be observations of the locations corrupted by additive noise:

$$\mathbf{y}_m(n+1) = \mathbf{C}\mathbf{x}_s(n+1) + \mathbf{v}(n+1) \tag{7}$$

where **C** is the measurement matrix and $\mathbf{v}(n)$ is the noise associated with the measurement process [*Zimmer*, 2011]. The measurement matrix, for the two-dimensional case has the form:

$$\boldsymbol{C} = \begin{bmatrix} 1 & 0 & 0 & 0 \\ 0 & 0 & 1 & 0 \end{bmatrix} \tag{8}$$

The Kalman filter uses the state space model defined by (4)-(7) to produce recursive estimates of the true positions contained in $\mathbf{x}_s(n)$ based on the observed measurements, $\mathbf{y}_m(n)$. In this case the measurement vector contains the estimated locations of the whale. In situations where the state evolution and measurement are linear and the stochastic processes are Gaussian then the Kalman filter yields the maximum *a posteriori* estimate of the states based on all of the measurements up to time n [*Arulampalam et al.*, 2002]. This is achieved by a two-step process, first a prediction step, wherein the estimates are updated based on the state model (4) and an update step in which the estimate is refined based on the new measurement. The updates for the Kalman filter can be written as [*Arulampalam et al.*, 2002]:

$$
\begin{aligned}
&\textit{Prediction step}:\\
&\hat{\boldsymbol{x}}_s(n+1|n) = \boldsymbol{A}\hat{\boldsymbol{x}}_s(n)\\
&\boldsymbol{P}(n+1|n) = \boldsymbol{A}\boldsymbol{P}(n|n)\boldsymbol{A}^t + \boldsymbol{Q}\\
&\textit{Update step}:\\
&\boldsymbol{\varepsilon}(n+1) = \boldsymbol{y}_m(n+1) - \boldsymbol{C}\hat{\boldsymbol{x}}(n+1|n)\\
&\boldsymbol{K}(n) = \boldsymbol{P}(n+1|n)\boldsymbol{C}^t(\boldsymbol{C}\boldsymbol{P}(n+1|n)\boldsymbol{C}^t + \boldsymbol{R})^{-1}\\
&\hat{\boldsymbol{x}}_s(n+1) = \hat{\boldsymbol{x}}_s(n+1|n) + \boldsymbol{K}(n)\boldsymbol{\varepsilon}(n+1)\\
&\boldsymbol{P}(n+1|n+1) = (\boldsymbol{I} - \boldsymbol{K}(n)\boldsymbol{C})\boldsymbol{P}(n+1|n) \qquad (9)
\end{aligned}
$$

where, in two dimensions $\mathbf{Q}$ (4×4) and $\mathbf{R}$ (2×2) are the correlation matrices of the Gaussian noise processes $\mathbf{w}(n)$ and $\mathbf{v}(n)$ respectively, which are provided to the algorithm. The quantities of the form $\hat{\boldsymbol{x}}_s$ are estimates of the state vector $\mathbf{x}_s(n)$. The notation "$(n+1|n)$" is used to represent estimates of a quantity at time $n+1$ based only on measurements up to time n, sometimes referred to as *a priori* estimates, accordingly notation of the form "$(n|n)$" denotes estimates of a quantity at time n based on all of the available measurements up to that time. The vector $\mathbf{K}(n)$ is called the Kalman gain and $\mathbf{P}$ (4×4) is an estimate of the correlation matrix for the errors in the state estimates, so provides information regarding the accuracy of the method. The state estimate is initialized using the first localisations and assuming a velocity of zero, whereas $\mathbf{P}(0)$ is initialised as the identity matrix $\mathbf{I}$.

3. Results

Detections

The dataset was very large (c. 300 Gb), so it was not feasible to run the location and tracking algorithms on the entire dataset. The detection algorithm was applied for periods of 1 hour on each day for four representative instruments (OBSs 13, 41, 45 and 51) in different parts of the study area (Fig. 3) to determine peak hours for whale vocalizations. There was a large variation in the hourly detection rate (Fig. 3). There were periods with low call rates on all four instruments, e.g., Julian days 156-170 and 213-215. Our analysis of the full dataset also showed that there were hours on particular days with very high call rates on multiple instruments, including days 175, 182 and 222. In addition, there was a high density of calls during the 16$^{\text{th}}$ hour of day 187 on OBS 41 and the 18$^{\text{th}}$ hour of day 182 on OBS 51. In summary, high call rates were found on multiple OBSs in the network over 1-2 hour periods on days 175, 179, 182, 187, 197 and 222. These peak hours are indications of fin whale presence in the area of the OBS array, and therefore likely to be identified on surrounding OBSs. These periods when large numbers of calls are detected presented the best opportunity of finding a sequence of vocalizations long enough to define a track. During days 156-174 and 197-212, when there was regular airgun shooting in the survey area, call detection rates were moderate, while outside these periods, rates were lower for some periods and higher for others (Fig. 3).

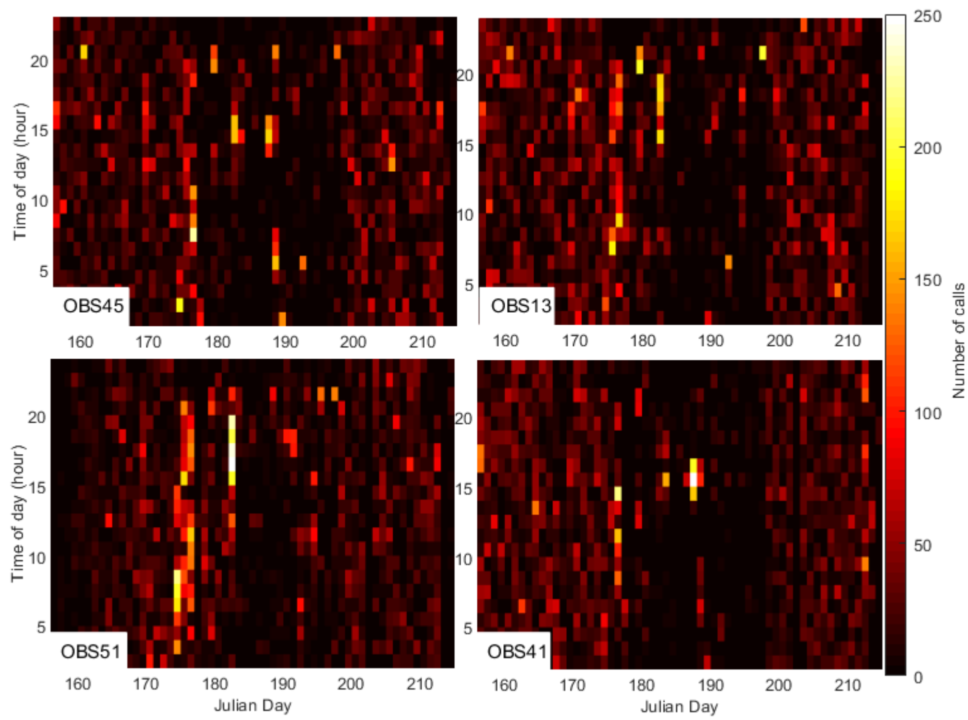

Figure 3: Hourly rates of call detection for four representative instruments during the time period covered by all four (see Fig. 4 for locations). The period of recording available varies between instruments.

Localization

Five tracks were constructed from stable sequences of 81-240 localisations during these periods (Fig. 4). On day 175, during the 80-minute period analysed, the whale initially travelled at an azimuth of c. 280° for c. 1 km and then turned approximately 100° clockwise to continue travelling at an azimuth of c. 020° for 1.7 km past OBS17. The mean velocity of the animal was around 2 km/hr. A track determined on day 179 covers a two-hour period, during which the whale travels backwards and forwards near OBS16 at an azimuth of c. 50° over a length of 4.5 km (Fig. 4). Many successive localisations are separated by distances that would represent impossible swim velocities and/or accelerations, but a linear fit of velocity against time results in velocities between 22 and 27 km/hr. A track on day 182 also covers a two-hour period, during which the whale travels 5 km at an azimuth of c. 20°, before turning to an azimuth of c. 80° for a further 3 km close to OBS51. The mean swim speed is 4 km/hr, but successive localisations indicate swim speeds of up to 24 km/hr for short periods. A track on day 187, close to OBS21, continues for a little less than one hour, during which the whale travelled c. 15 km. This track is more discontinuous than the others, suggesting that there were some rest periods. Swim speeds were generally between 10 and 20 km/hr. Localisations on day 197 were close to OBS29 and were too scattered to construct a coherent track. These calls occurred when airgun shooting was nearby, and we infer that the shots led either to false detections or to spurious cross-correlation maxima. Finally, a one-hour track was detected on day 222 near OBS64. The whale travelled to the northeast and then to the south, with a total track length of only 1.5 km and swim speed generally below 10 km/hr.

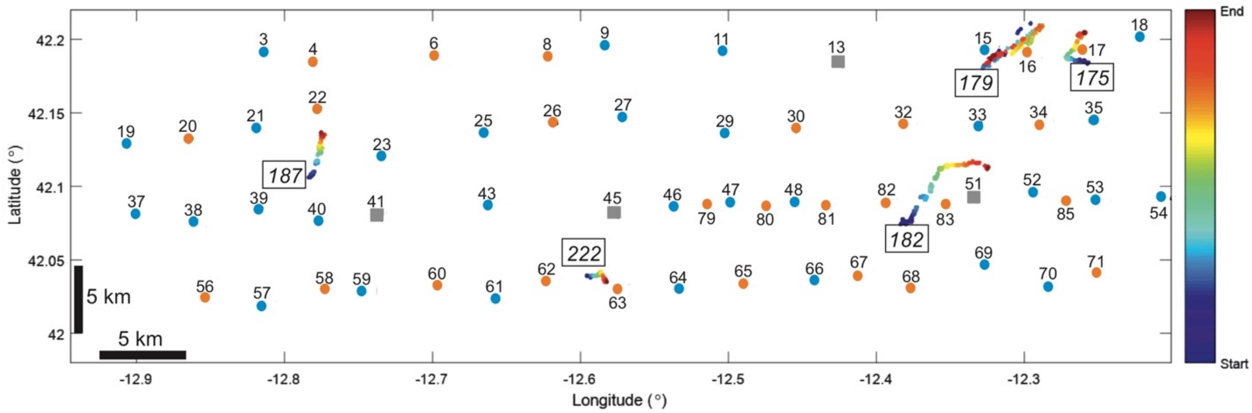

Figure 4: Fin whale tracks successfully followed. Colours on tracks mark an arbitrary time scale. Symbols mark OBS/OBH positions. Instrument locations marked with grey squares are those used for detection, blue circles are OBSs and orange circles are OBHs. Numbers in boxes mark the Julian day of each track.

To assess the uncertainties in these tracks, we analysed in further detail the track determined on day 175 (Fig. 5). A Monte-Carlo analysis [*White et al.*, 2006] applied to localisations using OBS13 as the reference instrument yielded 95% confidence ellipsoids with mean x and y dimensions of 39 m and 43 m, respectively (Fig. 5a). We also tested the sensitivity of inferred positions to the choice of reference instrument by re-computing the tracks using OBS/H 18, 35, 51, 52 and 54 as the reference instruments. Although the resulting tracks were all visually similar, Monte Carlo analysis of the combined results yielded 95% confidence ellipsoids with mean x and y dimensions of 325 m and 355 m respectively (Fig. 5b). Ellipsoid dimensions in the vertical plane were >100 m for both approaches, with some calls appearing to be above the ocean surface (perhaps due to our choice of sound speed profile), so it is clear that network geometries were not suitable for determining call depth.

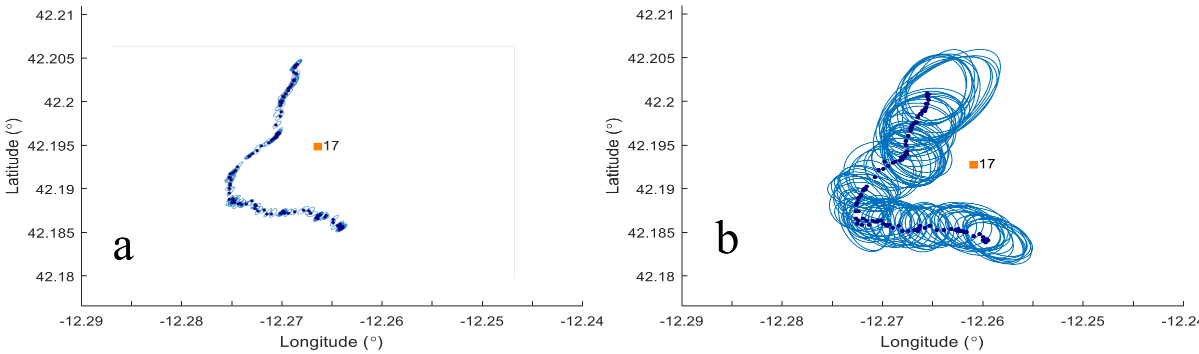

Figure 5: (a) Monte Carlo 95% confidence ellipses for localisations on day 175 when OBS13 is used as the reference instrument. (b) Corresponding confidence ellipses when localisations using six different OBH/S as reference instruments are combined.

One should note that when using multiple reference sensors the accuracy of the estimates degrades significantly. This may appear counter-intuitive, since using multiple reference sensors employs more sensor pairs, so one might anticipate a subsequent performance enhancement. Part of this location uncertainty comes from our simplification of the sound speed profile, which can result in range errors of up to a few hundred metres at the longest ranges, that are mitigated by the broad azimuthal distribution of OBSs used in localization. In addition, it should be noted that because the reference sensor used in the single reference sensor case is the sensor closest to the whale, all of the TDoA estimates are formed using at least one measurement with a high SNR. When using multiple reference sensors, there are some TDoA estimates which are formed when both sensors collect data with a relatively poor SNR. In those cases the TDoA estimates are unreliable and add considerable uncertainty to the location estimates, as seen in Fig. 5b.

Tracking

Because of the poor depth control, the Kalman filter was just applied in the horizontal plane, with the whale assumed to be at the ocean surface, consistent with previous suggestions that these animals dive no deeper than 50-100 m [*Croll et al.*, 2001; *Watkins et al.*, 1987]. The filter yielded very similar tracks to the localization method for all tracks. A representative example is shown in Fig. 6. However, it resulted in significant smoothing of calculated speeds, which are unrealistic if successive locations are used without filtering (Fig. 6b).

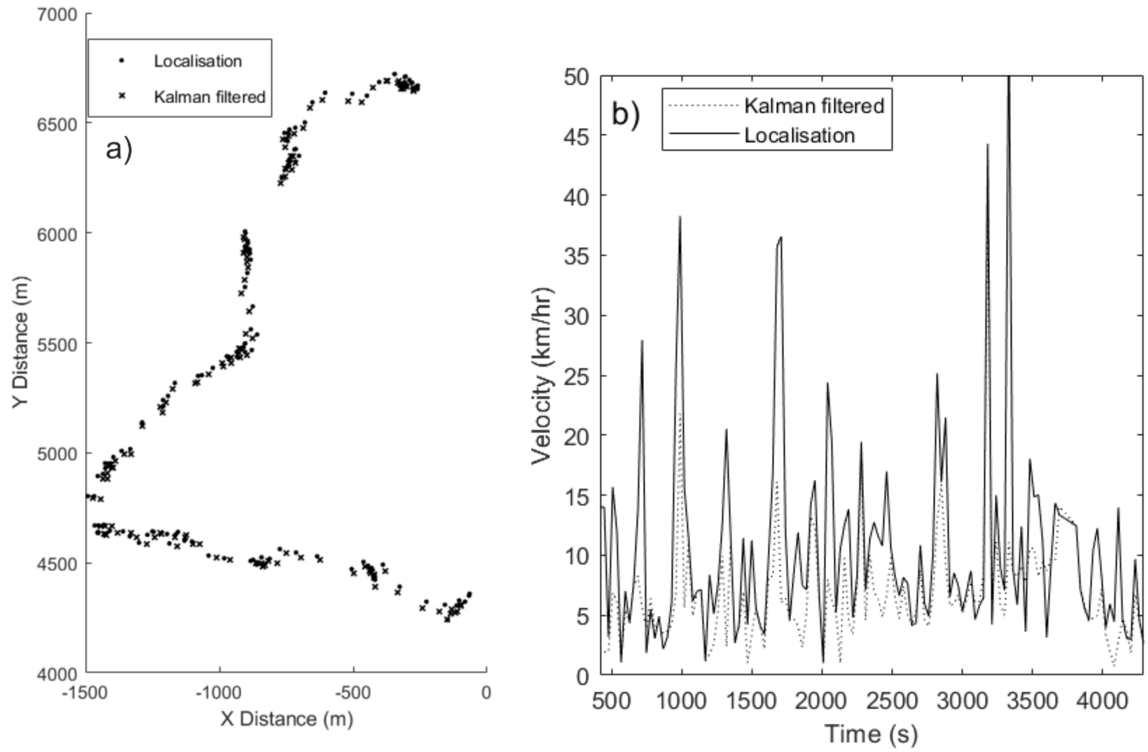

Figure 6: a) Comparison between tracks from localisation algorithm (filled circles) with those generated by the Kalman filter (crosses) for the track on day 175. b) Comparison of speed estimates based on localisation tracks with those from the Kalman filter for the track shown in a).

4. Discussion

We found no clear correlation between detection rate and the presence or absence of shooting. Other whale species have been found to increase the source level and frequency of their calling patterns to compensate for the presence of loud ambient noise [*Clark et al.*, 2002], but we cannot infer such a pattern from our data. No reliable whale tracks were recovered during the period of shooting, probably because of the low signal-to-noise ratio during these periods and the corresponding likelihood of spurious cross-correlation peaks.

Localizations were possible on six days with a range of success, over periods of 1-2 hours. Horizontal coordinates were recovered well, but we were not able to recover whale depths. The most continuous tracks were found on Julian days 175, 182, 187 and 222. The maximum error associated with these localizations was on the order of hundreds of metres, so significantly larger than the spacing between adjacent calls. Based on visual observations, swim speeds as high as 20 km/hr have been reported for a period of 20 mins [*Watkins*, 1981]. Using acoustic methods, *Dunn and Hernandez* [2009] estimated speeds of 3-7 km/hr. Using tags tracked by satellite, *Silva et al.* [2013] calculated mean swim speeds of 5.7 km/hr during foraging and 7.7 km/hr during migration, with large variations around these means. Recent work has showed that the swim speed of males is related to whether or not they are singing [*Clark et al.*, 2019] suggesting that singing animals mainly swim at slower speeds. In that study the mean swimming speed of all tracked whales was found to be 6.7 km/hr with a standard deviation of 3.7 km/hr. The mean swim speeds observed in this study correspond well with these data, although there are some point to point estimates that produce significantly higher values as a consequence of some remaining outliers in the localizations that the Kalman filter is unable to smooth sufficiently.

The tracks here cover periods up to 2 hours. The slow speeds estimated on days 175, 182 and 222, produce more meandering paths that are consistent with a singing male, whereas the changes in direction could be indicative of foraging behaviour [*Croll et al.*, 2001]. The track on day 187 is considerably faster and unidirectional, suggesting that the whale is showing a transiting behaviour. These two tracks types: transiting and meandering, are reported elsewhere *[McDonald et al., 1995; Rebull et al., 2006; Wilcock, 2012]* albeit in most of these instances the tracks are of longer duration.

5. Conclusions

We have used serendipitous recording of fin whale vocalisations during a deployment of 72 ocean bottom hydrophones/seismometers on the seabed with typical spacings of 4-6.5 km in c. 5 km water depth west of Iberia to locate their sources and ultimately to track several animals. From our analysis, we conclude the following:

1. Our call detection algorithm based on the ratios of signal strengths in different frequency bands appears to be highly successful in detecting the broad-band classic calls, but failed to detect a larger proportion of the narrower-band back-beats.
2. Analysis of a c. two-month time series for several representative instruments revealed up to c. 200 calls per hour,. There was no evidence that call detection rates were affected by the presence of airgun shooting.

3. In a few cases a series of calls lasting up to two hours was detected on enough seabed instruments to allow reliable estimation of time delays between instruments, and thus localisation and tracking. The use of a Kalman filter resulted in smoother tracks. Swim speeds along these tracks were highly variable, with means in the range 2-15 km/hr, and these variations may be linked to a variety of whale behaviours.
4. Long deployments of networks of fixed sound detectors on the seabed can provide rich datasets for the study of fin whale behaviour, but the detector spacing of 4-6 km used in our study limited our ability to locate and track the animals.

Acknowledgments:

Seabed instrument deployments were funded by the UK Natural Environment Research Council (NERC; grant NE/E016502/1) and by the Geomar Helmholtz Centre for Ocean Research Kiel. OBSs were provided and operated by the NERC Ocean Bottom Instrumentation Facility. We thank Dirk Klaeschen and the officers, crew and scientific parties of the research vessel *Poseidon* for their support at sea. We thank Jamie Burford, Masa Oue and Laura Gilling for their contributions to the development of the techniques used in this study, and Richard Davy for assistance with data access. We thank Luis Matias and an anonymous reviewer for their detailed and constructive comments. This work formed part of the University of Southampton Masters thesis of J. Fisher.

Black and white versions of colour figures

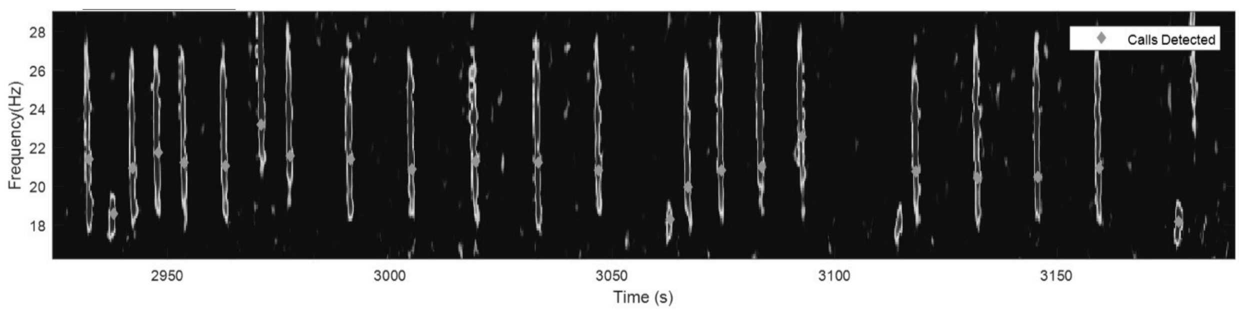

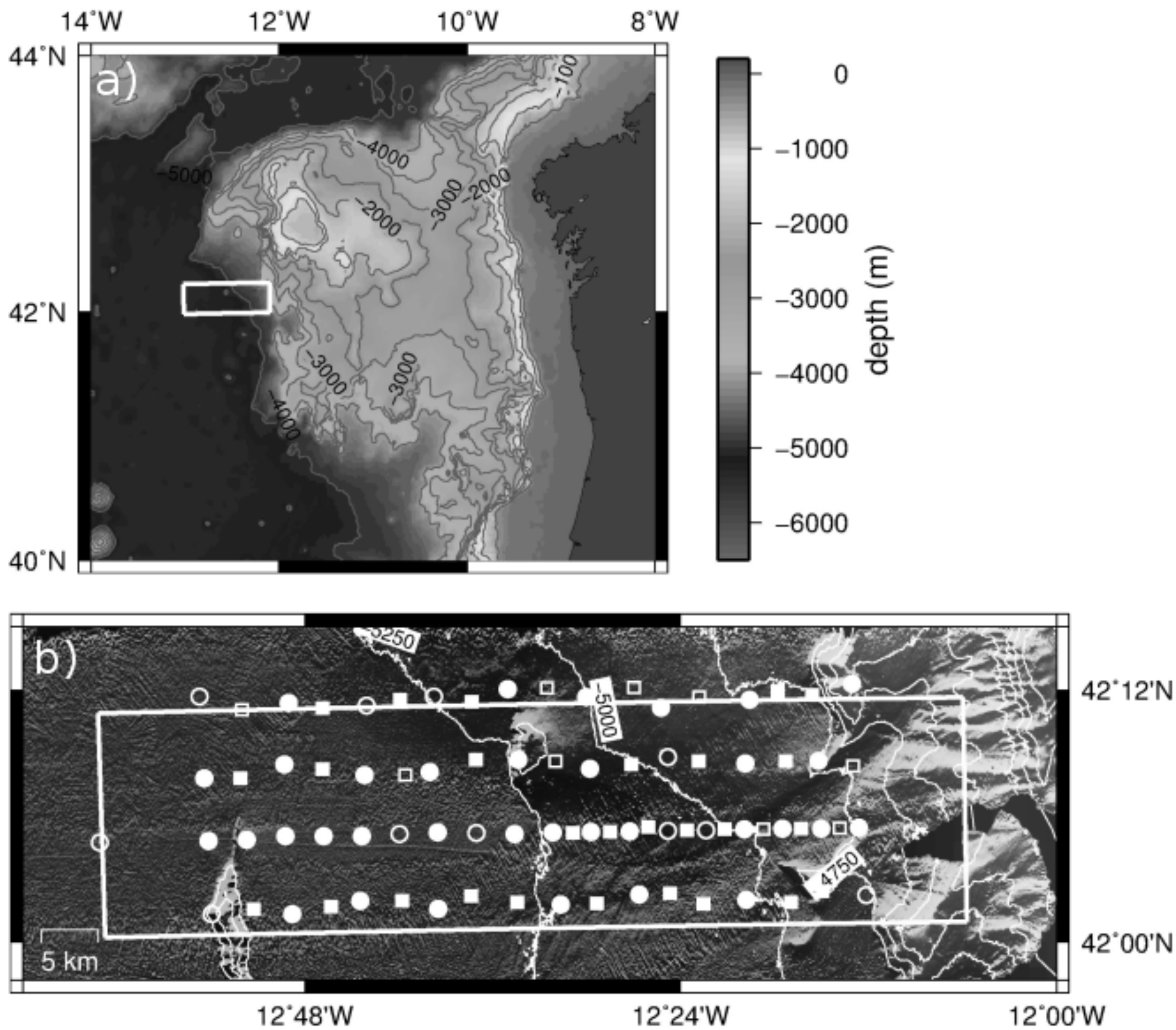

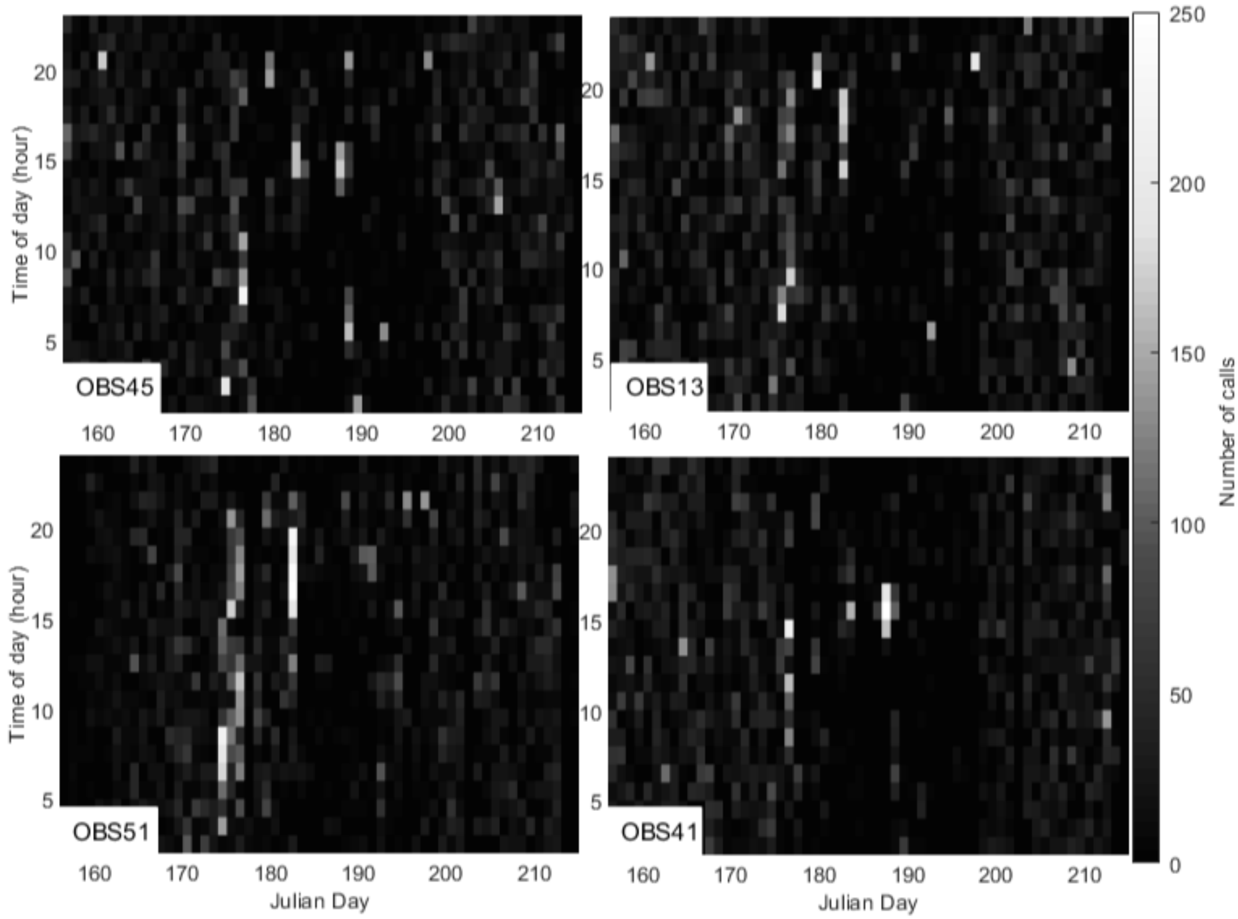

OBS45
OBS13
OBS51
OBS41
Time of day (hour)
Julian Day
Number of calls

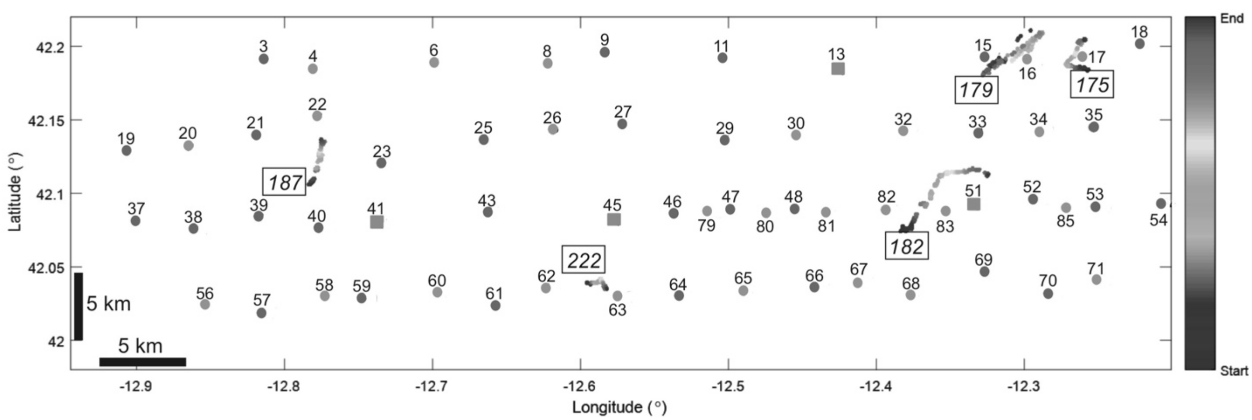

179
175
187
182
222
5 km
5 km
Latitude (°)
Longitude (°)
End
Start

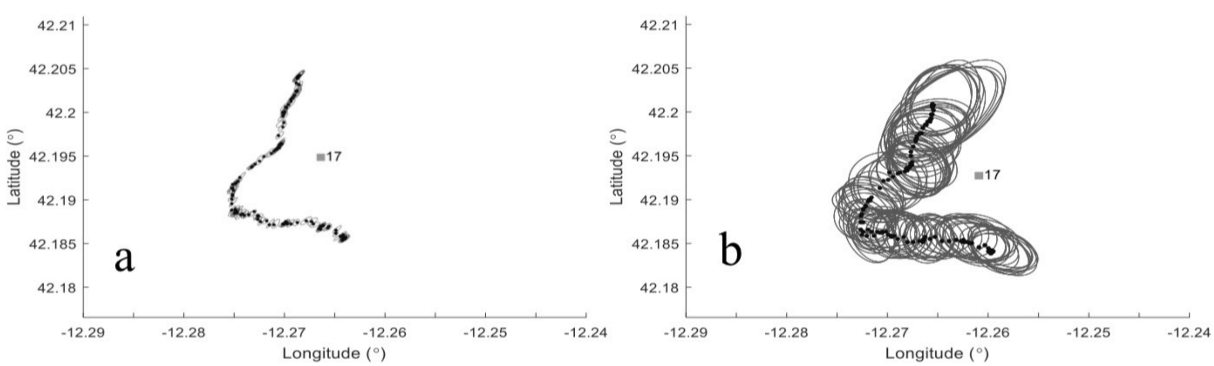

a
b
17
Latitude (°)
Longitude (°)

References

Arulampalam, M. S., S. Maskell, N. Gordon, and T. Clapp (2002), A tutorial on particle filters for online nonlinear/non-Gaussian Bayesian tracking, *Ieee Transactions on Signal Processing*, *50*(2), 174-188, doi:10.1109/78.978374.

Au, W. W., and M. O. Lammers (2016), *Listening in the Ocean*, Springer, doi:10.1007/978-1-4939-3176-7.

Baggenstoss, P. M. (2011), An algorithm for the localization of multiple interfering sperm whales using multi-sensor time difference of arrival, *J. Acoust. Soc. Am.*, *130*(1), 102-112, doi:10.1121/1.3598454.

Bayrakci, G., et al. (2016), Fault-controlled hydration of the upper mantle during continental rifting, *Nat. Geosci.*, *9*(5), 384-388, doi:10.1038/ngeo2671.

Bibby, J. M., and H. Toutenburg (1977), *Prediction and Improved Estimation in Linear Models*, Wiley, New York, doi:10.1002/bimj.197800029.

Castellote, M., C. W. Clark, and M. O. Lammers (2012), Fin whale (Balaenoptera physalus) population identity in the western Mediterranean Sea, *Mar. Mamm. Sci.*, *28*(2), 325-344, doi:10.1111/j.1748-7692.2011.00491.x.

Clark, C. W. (1995), Application of US Navy underwater hydrophone arrays for scientific research on whales, *Reports of the International Whaling Commission*, *45*, 210-212.

Clark, C. W., J. F. Borsani, and G. Notarbartolo-di-Sciara (2002), Vocal activity of fin whales, Balaenoptera physalus, in the Ligurian Sea, *Mar. Mamm. Sci.*, *18*(1), 286-295, doi:10.1111/j.1748-7692.2002.tb01035.x.

Clark, C. W., G. J. Gagnon, and A. S. Frankel (2019), Fin whale singing decreases with increased swimming speed, *Royal Society Open Science*, *6*(6), 180525, doi:doi:10.1098/rsos.180525.

Croll, D. A., A. Acevedo-Gutiérrez, B. R. Tershy, and J. Urbán-Ramírez (2001), The diving behavior of blue and fin whales: Is dive duration shorter than expected based on oxygen stores?, *Comparative Biochemistry and Physiology - A Molecular and Integrative Physiology*, *129*(4), 797-809, doi:10.1016/S1095-6433(01)00348-8.

Croll, D. A., C. W. Clark, A. Acevedo, B. Tershy, S. Flores, J. Gedamke, and J. Urban (2002), Bioacoustics: Only male fin whales sing loud songs - These mammals need to call long-distance when it comes to attracting females, *Nature*, *417*(6891), 809-809, doi:10.1038/417809a.

Davy, R. G., J. V. Morgan, T. A. Minshull, G. Bayrakci, J. M. Bull, D. Klaeschen, T. J. Reston, D. S. Sawyer, G. Lymer, and D. Cresswell (2018), Resolving the fine-scale velocity structure of continental hyperextension at the Deep Galicia Margin using full-waveform inversion, *Geophysical Journal International*, *212*(1), 244-263, doi:10.1093/gji/ggx415.

Dunn, R. A., and O. Hernandez (2009), Tracking blue whales in the eastern tropical Pacific with an ocean-bottom seismometer and hydrophone array, *J. Acoust. Soc. Am.*, *126*(3), 1084-1094, doi:10.1121/1.3158929.

Edds, P. L. (1988), Characteristics of finback balaenoptera physalus vocalizations in the St. Lawrence estuary, *Bioacoustics*, *1*(2-3), 131-149, doi:10.1080/09524622.1988.9753087.

Edds-Walton, P. L. (1997), Acoustic communication signals of mysticete whales, *Bioacoustics*, *8*(1-2), 47-60, doi:10.1080/09524622.1997.9753353.

Etter, P. C. (1995), *Underwater Acoustic Modeling: Principles, Techniques, and Applications*, 360 pp., CRC Press, London, UK.

Geijer, C. K. A., G. Notarbartolo di Sciara, and S. Panigada (2016), Mysticete migration revisited: are Mediterranean fin whales an anomaly?, *Mammal Review*, *46*(4), 284-296, doi:10.1111/mam.12069.
Harris, D. V., L. Matias, L. Thomas, J. Harwood, and W. H. Geissler (2013), Applying distance sampling to fin whale calls recorded by single seismic instruments in the northeast Atlantic, *The Journal of the Acoustical Society of America*, *134*(5), 3522-3535, doi:10.1121/1.4821207.
Harris, D. V., J. L. Miksis-Olds, J. A. Vernon, and L. Thomas (2018), Fin whale density and distribution estimation using acoustic bearings derived from sparse arrays, *The Journal of the Acoustical Society of America*, *143*(5), 2980-2993, doi:10.1121/1.5031111.
Hatch, L. T., and C. W. Clark (2004), Acoustic differentiation between fin whales in both the North Atlantic and North Pacific Oceans, and integration with genetic estimates of divergence, paper presented at International Whaling Commission Scientific Committee, Sorrento, Italy.
Iwase, R. (2015), Fin whale vocalizations observed with ocean bottom seismometers of cabled observatories off east Japan Pacific Ocean, *Japanese Journal of Applied Physics*, *54*(7S1), 07HG03, doi:10.7567/jjap.54.07hg03.
Kellogg, R. (1929), What is known of the migrations of some of the whale-bone whales, in *Annual Report of the Smithsonian Institution 1928*, edited, pp. 467-494, Washington, DC.
Knapp, C. H., and G. C. Carter (1976), The Generalized Correlation Method for Estimation of Time Delay, *IEEE Transactions on Acoustics, Speech, and Signal Processing*, *24*(4), 320-327, doi:10.1109/TASSP.1976.1162830.
Leung, T. S., and P. R. White (1998), Robust estimation of oceanic background spectrum, in *Mathematics in signal processing IV*, edited by J. G. McWhirty and I. K. Proudler, pp. 369-382, Clarendon Press, Oxford, doi:10.1007/BF00142586.
Li, X. R., and V. P. Jilkov (2003), Survey of maneuvering target tracking. Part I. Dynamic models, *IEEE Transactions on aerospace and electronic systems*, *39*(4), 1333-1364, doi:10.1109/TAES.2003.1261132.
Locke, J., and P. R. White (2011), The performance of methods based on the fractional Fourier transform for detecting marine mammal vocalizations, *J. Acoust. Soc. Am.*, *130*(4), 1974-1984, doi:10.1121/1.3631664.
Mahler, R. P. S. (2004), "Statistics 101" for multisensor, multitarget data fusion, *Ieee Aerospace and Electronic Systems Magazine*, *19*(1), 53-64, doi:10.1109/maes.2004.1263231.
Marple, S. L. (1999), Computing the discrete-time analytic signal via fft, *IEEE Transactions on Signal Processing*, *47*(9), 2600-2603, doi:10.1109/78.782222.
Matias, L., and D. Harris (2015), A single-station method for the detection, classification and location of fin whale calls using ocean-bottom seismic stations, *The Journal of the Acoustical Society of America*, *138*(1), 504-520, doi:10.1121/1.4922706.
McAulay, R. J., and M. L. Malpass (1980), Speech Enhancement Using a Soft-Decision Noise Suppression Filter, *IEEE Transactions on Acoustics, Speech, and Signal Processing*, *28*(2), 137-145, doi:10.1109/TASSP.1980.1163394.
McCarthy, E., D. Moretti, L. Thomas, N. DiMarzio, R. Morrissey, S. Jarvis, J. Ward, A. Izzi, and A. Dilley (2011), Changes in spatial and temporal distribution and vocal behavior of Blainville's beaked whales (Mesoplodon densirostris) during multiship exercises with mid-frequency sonar, *Mar. Mamm. Sci.*, *27*(3), E206-E226, doi:10.1111/j.1748-7692.2010.00457.x.
McDonald, M. A., J. A. Hildebrand, and S. C. Webb (1995), Blue and fin whales observed on a sea-floor array in the northeast Pacific, *J. Acoust. Soc. Am.*, *98*(2), 712-721, doi:10.1121/1.413565.

Mellinger, D. K., K. M. Stafford, S. E. Moore, R. P. Dziak, and H. Matsumoto (2007), An Overview of Fixed Passive Acoustic Observation Methods for Cetaceans, *Oceanography*, *20*(4), 36-45, doi:10.5670/oceanog.2007.03.
Minshull, T. A., M. C. Sinha, and C. Peirce (2005), Multi-disciplinary, sub-seabed geophysical imaging - A new pool of 28 seafloor instruments in use by the United Kingdom Ocean Bottom Instrument Consortium, *Sea Technology*, *46*(10), 27-31.
Moore, S. E., K. M. Stafford, D. K. Mellinger, and J. A. Hildebrand (2006), Listening for large whales in the offshore waters of Alaska, *Bioscience*, *56*(1), 49-55, doi:10.1641/0006-3568(2006)056[0049:Lflwit]2.0.Co;2.
Nguyen Hong Duc, P., D. Cazau, P. R. White, O. Gérard, J. Detcheverry, F. Urtizberea, and O. Adam (2021), Use of Ecoacoustics to Characterize the Marine Acoustic Environment off the North Atlantic French Saint-Pierre-et-Miquelon Archipelago, *Journal of Marine Science and Engineering*, *9*(2), 177, doi:10.3390/jmse9020177.
Nowacek, D. P., F. Christiansen, L. Bejder, J. A. Goldbogen, and A. S. Friedlaender (2016), Studying cetacean behaviour: new technological approaches and conservation applications, *Animal Behaviour*, *120*, 235-244, doi:10.1016/j.anbehav.2016.07.019.
Oleson, E. M., A. Slrovic, A. R. Bayless, and J. A. Hildebrand (2014), Synchronous Seasonal Change in Fin Whale Song in the North Pacific, *Plos One*, *9*(12), doi:10.1371/journal.pone.0115678.
Pereira, A., D. Harris, P. Tyack, and L. Matias (2020a), Fin whale acoustic presence and song characteristics in seas to the southwest of Portugal, *J. Acoust. Soc. Am.*, *147*(4), 2235-2249, doi:10.1121/10.0001066.
Pereira, A., D. Harris, P. Tyack, and L. Matias (2020b), On the use of the Lloyd's Mirror effect to infer the depth of vocalizing fin whales, *J. Acoust. Soc. Am.*, *148*(5), 3086-3101, doi:10.1121/10.0002426.
Perry, S. L., D. P. DeMaster, and G. K. Silber (1999), The great whales: History and status of six species listed as endangered under the U.S. Endangered Species Act of 1973, *Marine Fisheries Review*, *61*(1), 1-74.
Rebull, O., G., J. D. Cusí, M. Ruiz Fernández, and J. G. Muset (2006), Tracking fin whale calls offshore the Galicia Margin, North East Atlantic Ocean, *J. Acoust. Soc. Am.*, *120*(4), 2077-2085, doi:10.1121/1.2336751.
Schuba, C. N., G. G. Gray, J. K. Morgan, D. S. Sawyer, D. J. Shillington, T. J. Reston, J. M. Bull, and B. E. Jordan (2018), A low-angle detachment fault revealed: Three-dimensional images of the S-reflector fault zone along the Galicia passive margin, *Earth Planet. Sci. Lett.*, *492*, 232-238, doi:10.1016/j.eps1.2018.04.012.
Silva, M. A., R. Prieto, I. Jonsen, M. F. Baumgartner, and R. S. Santos (2013), North Atlantic Blue and Fin Whales Suspend Their Spring Migration to Forage in Middle Latitudes: Building up Energy Reserves for the Journey?, *PLoS ONE*, *8*(10), doi:10.1371/journal.pone.0076507.
Širović, A., J. A. Hildebrand, and S. M. Wiggins (2007), Blue and fin whale call source levels and propagation range in the Southern Ocean, *J. Acoust. Soc. Am.*, *122*(2), 1208-1215, doi:10.1121/1.2749452.
Sirovic, A., L. N. Williams, S. M. Kerosky, S. M. Wiggins, and J. A. Hildebrand (2013), Temporal separation of two fin whale call types across the eastern North Pacific, *Mar. Biol.*, *160*(1), 47-57, doi:10.1007/s00227-012-2061-z.

Stafforda, K. M., D. K. Mellinger, S. E. Moore, and C. G. Fox (2007), Seasonal variability and detection range modeling of baleen whale calls in the Gulf of Alaska, 1999-2002, *J. Acoust. Soc. Am.*, *122*(6), 3378-3390, doi:10.1121/1.2799905.
Stimpert, A. K., et al. (2015), Sound production and associated behavior of tagged fin whales (Balaenoptera physalus) in the Southern California Bight, *Animal Biotelemetry*, *3*(1), doi:10.1186/s40317-015-0058-3.
Thompson, P. O., L. T. Findley, and O. Vidal (1992), 20-Hz pulses and other vocalizations of fin whales, Balaenoptera-physalus, in the Gulf of Mexico, *J. Acoust. Soc. Am.*, *92*(6), 3051-3057, doi:10.1121/1.404201.
Watkins, W. A. (1981), Activities and underwater sounds of fin whales, *Sci. Rep. Whales Res. Inst*, *33*, 83-117.
Watkins, W. A., P. Tyack, K. E. Moore, and J. E. Bird (1987), The 20-Hz signals of finback whales (Balaenoptera-Physalus), *J. Acoust. Soc. Am.*, *82*(6), 1901-1912, doi:10.1121/1.395685.
Weirathmueller, M. J., W. S. D. Wilcock, and D. C. Soule (2013), Source levels of fin whale 20 Hz pulses measured in the Northeast Pacific Ocean, *J. Acoust. Soc. Am.*, *133*(2), 741-749, doi:10.1121/1.4773277.
White, P. R., T. G. Leighton, D. C. Finfer, C. Powles, and O. N. Baumann (2006), Localisation of sperm whales using bottom-mounted sensors, *Appl. Acoust.*, *67*(11-12), 1074-1090, doi:10.1016/j.apacoust.2006.05.002.
Wiggins, S. M., and J. A. Hildebrand (2007), High-frequency Acoustic Recording Package (HARP) for broad-band, long-term marine mammal monitoring, in *2007 Symposium on Underwater Technology and Workshop on Scientific Use of Submarine Cables and Related Technologies, Vols 1 and 2*, edited, pp. 551-557, doi:10.1109/UT.2007.370760.
Wilcock, W. S. D. (2012), Tracking fin whales in the northeast Pacific Ocean with a seafloor seismic network, *J. Acoust. Soc. Am.*, *132*(4), 2408-2419, doi:10.1121/1.4747017.
Zimmer, W. M. X. (2011), *Passive acoustic monitoring of cetaceans*, 1-356 pp., doi:10.1017/CBO9780511977107.